Brazilian Journal of Physics
ISSN: 0103-9733
luizno.bjp@gmail.com
Sociedade Brasileira de Física
Brasil

Grams, Guilherme; Santos, Alexandre M.; Menezes, Debora P.
Equation of State Grid with the Quark-Meson-Coupling Model
Brazilian Journal of Physics, vol. 46, núm. 1, febrero, 2016, pp. 111-119
Sociedade Brasileira de Física
São Paulo, Brasil

Braz J Phys (2016) 46:111–119
DOI 10.1007/s13538-015-0386-z

SOCIEDADE BRASILEIRA DE FÍSICA

NUCLEAR PHYSICS

Equation of State Grid with the Quark-Meson-Coupling Model

Guilherme Grams[1] · **Alexandre M. Santos**[1] · **Débora P. Menezes**[1]

Received: 20 August 2015 / Published online: 17 November 2015

Abstract In this work, we present the preliminary results of an equation of state (EoS) grid for possible use in core-collapse supernova simulations. We treat uniform matter made of nucleons using the quark-meson coupling (QMC) model. We show a table with a variety of thermodynamic quantities, which covers the proton fraction range $Y_p = 0-0.65$ with the linear grid spacing $\Delta Y_p = 0.01$ (66 points) and the density range $\rho_B = 10^{14} - 10^{16}$g cm^{-3} with the logarithmic grid spacing $\Delta \log_{10}(\rho_B/[\text{g cm}^{-3}]) = 0.1$ (21 points). This preliminary study is performed at zero temperature, and our results are compared with the widely used EoS already available in the literature.

Keywords Equation of state · Quark-meson-coupling · Nuclear · Supernova

1 Introduction

Although the theory related to supernova (SN) has made a remarkable progress in the past decade, there are many questions that remain unanswered. The catastrophic infall of the core of a massive star, reversed to trigger the powerful ejection of the stellar mantle and envelope in a supernova explosion, plays a crucial role in the synthesis of heavy elements. But when, why, and how it happens is a fundamental problem of stellar astrophysics that remains to be explained. The implosion of stellar cores was also proposed as part of the scenario of the stellar death [1, 2].

✉ Guilherme Grams
grams.guilherme@gmail.com

[1] Universidade Federal de Santa Catarina, Florianópolis, Brazil

There are no doubts that supernovae explosions are an unique phenomenon in nature and an excellent laboratory to test extreme physics conditions. Core-collapse SNe tend to happen once every $\sim 30 - 50$ years in our galaxy and unfortunately most part of them are shrouded from view by the dust that pervades the Milk Way [3] which makes the study of these *great labs* very difficult. Due to this observational difficulty, simulations of core-collapse supernova have played an important role in the study of supernovae explosions and their possible remnants. The equation of state (EoS) of nuclear physics is a fundamental ingredient in the simulation of SN explosion. Simulations of core-collapse supernovae depend on the EoS obtained for a wide range of thermodynamic conditions. Moreover, extremely high density and temperature may be achieved when black holes are formed by failed supernovae. The temperatures of interest vary from zero to more than 100 MeV, densities range go from 10^5 to more than 10^{15} g cm^{-3} and the proton fraction can reach 0.6. Fulfilling these conditions makes the construction of a complete EoS a very hard work, mainly at low densities, where a variety of substructures and light clusterization are possible. For these reasons, there are only few complete EoS available in the literature. The most commonly used EoS are those of Lattimer and Swesty (hereafter LS) [4], Shen et al. (hereafter STOS) [5, 6] and Hempel and Schaffner-Bielich (hereafter HS) [7].

The LS [4] EoS is based on a compressible liquid drop model with a Skyrme force for nucleon interactions. The STOS EoS from 1998 [5] was the first equation of state for supernova simulations using a relativistic nuclear model. The upgrade to STOS's work was published in 2011 [6] with more points in the table and the inclusion of the Λ hyperons. Both works developed by STOS were constructed with the TM1 [8] parameterization of the relativistic nonlinear

Walecka model, developed in [9, 10] and also called Boguta-Bodmer type model, in a mean field approximation.

HS's EoS [7] is based on the NL3 [11], TM1, TMA [12], FSUgold [13], SFHo and SFHx [14], IU-FSU [15] and DD2 [16] parameterizations of the same quantum hadrodynamics model and use the nuclear statistical equilibrium model of HS and Schaffner-Bielich [17], which takes into account excluded volume effects.

An interesting analysis of the different parameterizations of the relativistic-mean-field (RMF) models was made by Dutra et al. [18], where the authors analyzed 263 different RMF models under several constrains related to the symmetric nuclear matter (SNM) and pure neutron matter (PNM). The TM1 parameterization used by STOS failed under six of this constraints. The parameterizations used by HS: TMA, FSUgold, NL3, IU-FSU, and DD2 failed under five, one, nine, two, and three constraints, respectively. The parameterizations SFHo and SFHx were not analyzed in [18].

The works of HS, LS, and STOS were successful and very useful in many calculations in the last decade [19–24], but there are some simulations of SN in which the supernova does not explode [25].

One of the problems that can cause these failures is the use of an inadequate or incomplete nuclear EoS. The EoS of dense matter determines the stellar structure, the hydrodynamics, and the reaction rates through the calculation of pressure, entropy, and chemical compositions [26, 27]. Sumiyoshi et al. [28] performed numerical simulations of core-collapse supernovae. They examined the influence of the equation of state on the postbounce evolution of shock waves in the late phase and the resulting thermal evolution of protoneutron stars with two different EoS, namely LS and STOS. None of them resulted in a successful explosion of the supernova core. When the central core contracts to become a protoneutron star, differences due to different EoSs appear. The central density becomes very high and the chosen EoS may influence the shock dynamics and the consequent evolution to a protoneutron star cooling or to the formation of a black hole [28].

In the present work, we present our preliminary results for the construction of an EoS grid for core-collapse supernova simulations, with the quark-meson coupling (QMC) model [29]. In the QMC model, nuclear matter is described as a system of non-overlapping MIT bags [30] that interact through the exchange of scalar and vector meson fields. Many applications and extensions of the model have been made in the last years [31–35]. It is well known that the EoS for infinite nuclear matter at zero temperature derived from the QMC model is softer than many of the EoS obtained with quantum hydrodynamical models with nonlinear terms [9]. This might be a problem if one wants to describe very massive compact objects [36, 37], and we tackle how to circumvent this problem after our results are presented. However, as far as SN simulations are concerned, it is worth testing the QMC model because of its underlying quark substructure. Moreover, the effective nucleon mass obtained with the QMC model lies in the range 0.7–0.8 of the free nucleon mass, which agrees with the results derived from the non-relativistic analysis of scattering of neutrons from lead nuclei [38] and is larger in comparison with the effective mass obtained with some of the different parameterizations of the Boguta-Bodmer models. A low effective mass at saturation can be a problem when hyperons are included in the calculation, as discussed in the next section.

In the relativistic EoS mentioned in the beginning of this section that were obtained to be used in SN simulations, the nucleons interact among themselves through the exchange of mesons. We believe that with the quarks degree of freedom present in the QMC model, a more fundamental physics not present in the other models, can be tested and possibly contribute for the SN simulations to explode.

Another possible use of this preliminary EoS obtained with the QMC model is the study of the cooling of compact stars, which serve as an important window on the properties of super-dense matter and neutron star structure, and is very sensitive to the nuclear equation of state [39–42].

This paper is structured as follows: in the second section, we present a review of the quark-meson coupling model. In the third section, we present our results for the EoS. The last section is reserved for the final remarks and conclusions.

2 The Quark-Meson Coupling Model

In the QMC model, the nucleon in nuclear medium is assumed to be a static spherical MIT bag in which quarks interact with the scalar (σ) and vector (ω, ρ) fields, and those are treated as classical fields in the mean field approximation (MFA) [29]. The quark field, ψ_{q_N}, inside the bag then satisfies the equation of motion:

$$\left[i\not{\partial} - (m_q^0 - g_\sigma^q) - g_\omega^q \omega \gamma^0 + \frac{1}{2} g_\rho^q \tau_z \rho_{03} \gamma^0\right] \psi_{q_N}(x) = 0 \ , \quad q = u, d \tag{1}$$

where m_q^0 is the current quark mass, and g_σ^q, g_ω^q, and g_ρ^q denote the quark-meson coupling constants. The normalized ground state for a quark in the bag is given by

$$\psi_{q_N}(\mathbf{r}, t) = \mathcal{N}_{q_N} \exp\left(-i\epsilon_{q_N} t / R_N\right) \times \begin{pmatrix} j_{0_N}\left(x_{q_N} r / R_N\right) \\ i\beta_{q_N} \vec{\sigma} \cdot \hat{r}\, j_{1_N}\left(x_{q_N} r / R_N\right) \end{pmatrix} \frac{\chi_q}{\sqrt{4\pi}} \ , \tag{2}$$

where

$$\epsilon_{q_N} = \Omega_{q_N} + R_N \left(g_\omega^q \, \omega + \frac{1}{2} g_\rho^q \tau_z \rho_{03} \right), \tag{3}$$

and,

$$\beta_{q_N} = \sqrt{\frac{\Omega_{q_N} - R_N \, m_q^*}{\Omega_{q_N} + R_N \, m_q^*}}, \tag{4}$$

with the normalization factor given by

$$\mathcal{N}_{q_N}^{-2} = 2R_N^3 \, j_0^2(x_q) \left[\Omega_q(\Omega_q - 1) + R_N m_q^*/2 \right] \Big/ x_q^2 , \tag{5}$$

where $\Omega_{q_N} \equiv \sqrt{x_{q_N}^2 + (R_N \, m_q^*)^2}$, $m_q^* = m_q^0 - g_\sigma^q \, \sigma$, R_N is the bag radius of nucleon N and χ_q is the quark spinor. The bag eigenvalue for nucleon N, x_{q_N}, is determined by the boundary condition at the bag surface

$$j_{0_N}(x_{q_N}) = \beta_{q_N} \, j_{1_N}(x_{q_N}) . \tag{6}$$

The energy of a static bag describing nucleon N consisting of three quarks in ground state is expressed as

$$E_N^{\text{bag}} = \sum_q n_q \, \frac{\Omega_{q_N}}{R_N} - \frac{Z_N}{R_N} + \frac{4}{3} \pi \, R_N^3 \, B_N , \tag{7}$$

where Z_N is a parameter which accounts for zero-point motion of nucleon N and B_N is the bag constant. The set of parameters used in the present work is determined by enforcing stability of the nucleon (here, the "bag"), like in [43], so there is a single value for proton and neutron masses. The effective mass of a nucleon bag at rest is taken to be $M_N^* = E_N^{\text{bag}}$.

The equilibrium condition for the bag is obtained by minimizing the effective mass, M_N^* with respect to the bag radius

$$\frac{d \, M_N^*}{d \, R_N^*} = 0, \quad N = p, n, \tag{8}$$

By fixing the bag radius $R_N = 0.6$ fm and the bare nucleon mass $M = 939$ MeV, one can set the values for the unknowns Z_N and $B^{1/4}$. In our calculations, we have found $Z_N = 4.0050668$ and $B_N^{1/4} = 210.85$MeV. Furthermore, the desired values of $B/A \equiv \epsilon/\rho - M = -15.7$ MeV at saturation $n = n_0 = 0.15$ fm^{-3} are achieved by setting $g_\sigma^q = 5.9810$, $g_\omega = 8.9817$, where $g_\omega = 3g_\omega^q$ and $g_\rho = 3g_\rho^q$. All the parameters used in this work are shown in Table 1.

The total energy density of the nuclear matter reads

$$\varepsilon = \frac{1}{2} m_\sigma^2 \sigma + \frac{1}{2} m_\omega^2 \omega_0^2 + \frac{1}{2} m_\rho^2 \rho_{03}^2 + \sum_N \frac{1}{\pi^2} \int_0^{k_N} k^2 dk [k^2 - M_N^{*2}]^{1/2}, \tag{9}$$

Table 1 Parameters used in the QMC model and different parameterizations of the Boguta-Bodmer type models

Model	M (MeV)	m_q (MeV)	m_σ (MeV)	m_ω (MeV)	m_ρ (MeV)	g_ρ	g_ω	g_σ	$B_N^{1/4}$ (MeV)	NLT	DDP
QMC	939.0	5.5	550	783	770	8.651	8.9817	5.9810*	210.85	no	no
NL3	939.0	–	508.194	782.501	763	8.9480	12.868	10.217	–	yes	no
GM1	939.0	–	550	783	770	8.1945	10.608	9.5684	–	yes	no
TM1	938.0	–	511.197	783	770	4.6321	12.613	10.028	–	yes	no
FSUgold	939.0	–	491.5	782.5	763	11.7673	14.301	10.592	–	yes	no
SFHo	939.0	–	467.94	726.5	770	11.443	10.8144	15.123	–	yes	no
SFHx	939.0	–	470.51	726.5	770	11.5153	12.2438	16.1868	–	yes	no
IU-FSU	939.0	–	491.5	782.5	763	8.92188	12.8679	10.217	–	yes	no
TMA†	938.9	–	519.151	781.95	768.1	3.800	12.842	10.055	–	yes	no
DD2	939.0	–	546.212	783	763	3.62694**	13.3424**	10.687**	–	no	yes
TW	939.0	–	550	783	763	7.32196**	13.2901**	10.728**	–	no	yes

In the first line we present the parameters used in the present work for the QMC model. The NL3, GM1, and TW parameterizations are used here for a comparison of bulk matter properties. TM1 is the parameterization used in STOS's work. The FSUgold, SFHo, SFHx, IU-FSU, TMA, and DD2 were used in HS's work.

* g_σ^q is the quark-meson coupling in the QMC model.

** values taken at saturation for the DDP parameterizations.

TMA†: the coupling parameters g_i of the set TMA are chosen to be mass-number dependent such that $g_i = a_i + b_i/A^{0.4}$, with a_i and b_i being constants [12]; for infinite matter as in the stellar matter, one has an infinite nucleus, and then the limit A $\mapsto$ infinity is taken so that $g_i = a_i$. NLT= Nonlinear terms. DDP= Density dependent parameters

Table 2 Nuclear matter bulk properties obtained with the QMC model, two different parameterizations of the Boguta-Bodmer model and one density dependent model we use in this paper, and the seven parameterizations used in the works of HS and STOS. All quantities are taken at saturation

Model	B/A (MeV)	n_0 (fm^{-3})	M^*/M	$\mathcal{E}_{sym}$ (MeV)	K (MeV)
QMC	-15.7	0.150	0.77	34.5	295
NL3	-16.2	0.148	0.60	37.4	272
GM1	-16.3	0.153	0.70	32.5	300
TM1	-16.3	0.145	0.63	36.8	281
FSUgold	-16.3	0.148	0.62	32.6	230
SFHo	-16.2	0.158	0.76	31.6	245
SFHx	-16.2	0.160	0.72	28.7	239
IU-FSU	-16.4	0.155	0.61	31.3	231
TMA	-16.0	0.147	0.63	30.7	318
DD2	-16.0	0.149	0.56	31.7	243
TW	-16.2	0.153	0.56	32.6	240

and the pressure is

$$p = -\frac{1}{2}m_\sigma^2\sigma + \frac{1}{2}m_\omega^2\omega_0^2 + \frac{1}{2}m_\rho^2\rho_{03}^2 + \sum_N \frac{1}{\pi^2}\int_0^{k_N} k^4 dk/[k^2 - M_N^{*2}]^{1/2}. \quad (10)$$

The vector mean field ω_0 and ρ_{03} are determined through

$$\omega_0 = \frac{g_\omega(n_p + n_n)}{m_\omega^2}, \quad \rho_{03} = \frac{g_\rho(n_p - n_n)}{m_\rho^2}, \quad (11)$$

where

$$n_B = \sum_N \frac{2k_N^3}{3\pi^2}, \quad N = p, n. \quad (12)$$

is the baryon density.

Finally, the mean field σ is fixed by imposing that

$$\frac{\partial \varepsilon}{\partial \sigma} = 0. \quad (13)$$

It is always important to check the behavior of the models in the symmetric nuclear matter at saturation density and zero temperature, i.e., the bulk nuclear matter properties. A comprehensive work in this direction is found in [18], but the QMC model was not analyzed. Therefore, we compare the QMC model with two parameterizations of the well known hadrodynamical models [9, 44], namely, GM1 [45] and NL3 [11] and the density-dependent parameter (DDP) model TW [46]. In this work, we have chosen GM1 for being a parameterization which gives reasonable stellar macroscopic properties, NL3 because it is commonly used parameterization in the literature and TW because it is a very good density-dependent parameterization according to [18]. In [18], it was found that GM1 fails in the comparison with six constrains related to the symmetric nuclear matter (SNM) and pure neutron matter (PNM), NL3 fails in nine of them and TW satisfies all constraints but one.

In Table 1, we can see the different parameters here analyzed and the ones used in the works of STOS [5, 6] and HS [7].

In Table 2, we show the properties of nuclear matter at saturation density and zero temperature. The first column shows the binding energy per nucleon, the second shows the baryonic density of the nucleons at the saturation point, and the third shows the effective mass relative to the free nucleon mass, the symmetry energy, and the compression modulus of the nucleons.

In Fig. 1, we show the relation of the effective mass as function of the baryonic density. We can see that the effective mass for the QMC model has always a larger value than the other models, which is an important characteristic

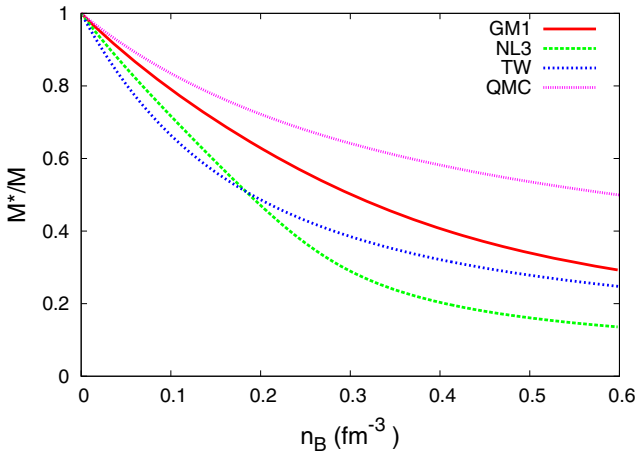

Fig. 1 The effective mass of the QMC model, the two Boguta-Bodmer parameterizations and the DDP model

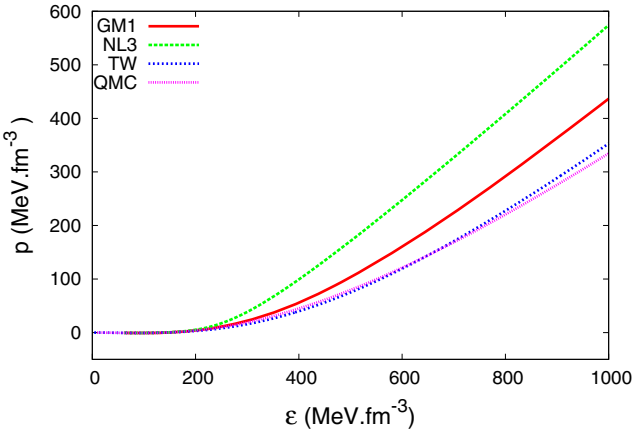

Fig. 2 Equations of state for symmetric matter obtained with the QMC model, the two Boguta-Bodmer parameterizations and the DDP model

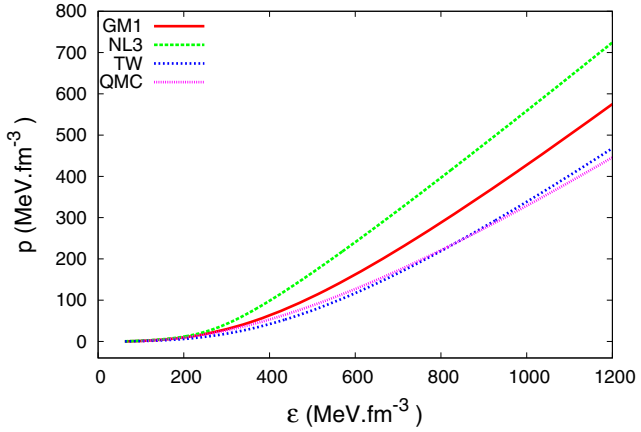

Fig. 3 Equations of state in beta equilibrium obtained from the QMC model, the two Boguta-Bodmer parameterizations and the DDP model

if hyperons are to be included. As can be seen in [47], the effective mass of some of the Boguta-Bodmer-type models tend to zero at still low densities when all the baryons of the octet are included. For this reason, parameterizations with larger effective masses were proposed by Glendenning [45] (GM1, GL, etc) with the specific purpose of applications to stellar matter. The QMC model gives $M^*/M = 0.77$ at the saturation density, which agrees with the results derived from the non-relativistic analysis of scattering of neutrons from lead nuclei [38]. This result is larger in comparison with the effective masses obtained from many of the quantum hadrodynamical models, as can be seen in Table 2.

In Fig. 2, we show the pressure versus the energy density for infinite nuclear matter at $T = 0$, where we see that the curve obtained within the QMC model is similar to the one for TW and softer than the ones obtained with the GM1 and NL3 parameterizations.

Besides the bulk nuclear matter, it is also interesting to test the QMC model in the study of neutron star properties. In stellar matter, charge neutrality and beta equilibrium have to be enforced. Thereafter, we plot in Fig. 3 the equation of state for stellar matter. We can see that the curve for the QMC is softer than the others. However, as seen in Table 3, the QMC model gives a maximum mass for a neutron star bigger than two solar masses, in agreement with recent observational results of [36, 37].

We are aware that if we include hyperons in the EoS the maximum mass will be lowered. However, there are some ways to control this shortcoming. One usual method to make the EoS stiffer, without altering its properties below the nuclear saturation density, is to consider strange meson fields in the Lagrangian density and choose the hyperon-meson couplings such as that the appearance of strange hyperons are pushed toward high densities [48–50]. Recently, another alternative was proposed by [51], where the authors force the σ self-interaction potential to rise abruptly in densities a bit larger than the nuclear saturation density, which results in a stiffer EoS, and consequently, the maximum possible stellar mass increases.

It is important to notice that this is a preliminary work towards the construction of a complete equation of state that in the future can be used to simulate core-collapse supernova explosions. According to [14], the concept of *soft* or *stiff* EoS, normally used in neutron star studies, may not apply here. The authors pointed out that as core-collapse SN explores a large range of densities and temperatures, an EoS which has a higher pressure at one density and temperature may have a lower pressure at another density and temperature.

3 Results and Discussions

We next construct an EoS table covering a wide range of proton fractions Y_p and baryon densities n_B. We show only some of the results related to the properties of matter with the QMC model and indicate the website from where the full table can be download.

We show in Fig. 4 the binding energy of homogeneous nuclear matter at zero temperature as a function of the baryon density for different proton fractions. For pure neutron matter and low proton fractions, there are no binding states, as expected. This result is in good agreement with Walecka [44] and STOS [5]. In Fig. 5, we show the compression modulus versus the baryonic density, where K is given by:

$$K = 9\, n_B^2 \frac{d^2}{dn_B^2}\left(\frac{\varepsilon}{n_B}\right), \tag{14}$$

n_B is the baryon number density and ε the total energy density of the nucleons. One can see that up to two times

Table 3 The first column of data shows the maximum star mass of each model. The second shows the respective radii. The third, the central energy density for such maximum mass and respective radius

Model	M_{max} (M_0)	R (Km)	ε_0 (fm^{-4})
QMC	2.13	11.12	6.33
GM1	2.35	12.09	4.43
NL3	2.79	12.99	4.39
TW	2.07	10.61	6.27

nuclear saturation density, the compression modulus is practically independent of the proton fraction. It increases with the increase of the proton fraction only at higher densities.

In Fig. 6, the pressure p as a function of ρ_B is displayed. The baryon number density is related to the baryon mass density as $\rho_B = m_u n_B$ where $m_u = 931.49432$ MeV is the atomic mass unit. The pressure varies more with the Y_p for low values of p and lower densities, a result which is in good agreement with STOS's work [5].

In Fig. 7, we show the proton and neutron chemical potentials, μ_p and μ_n, as function of the baryon density for different proton fractions. We see that for $Y_p = 0.1$, the chemical potential of the neutron is bigger than the one of the proton. As the proton fraction gets bigger, the curves approach each other, until they are the same in $Y_p = 0.5$, and for $Y_p = 0.6$ the chemical potential of the proton is bigger than the one of the neutron. This is an obvious result, but as the chemical potentials are very important quantities in the EoS tables, they are also presented graphically.

Once bulk nuclear matter properties are shown to behave as expected and present some important differences as compared with the other works, we proceed toward building a preliminary EoS table with the QMC model, for homogeneous matter and zero temperature, which is available on the Web at http://debora.fsc.ufsc.br/eos_qmc.t0.

In Table 4, we show the thermodynamic quantities described as in [5, 6]

1. Temperature: T [MeV].
2. Logarithm of baryon mass density: $\log_{10}(\rho_B)$[g cm^{-3}].
3. Baryon number density: n_B [fm^{-3}].
4. Proton fraction: Y_p.
   The proton fraction Y_p of uniform matter made of protons and neutrons is defined by
   $$Y_p = \frac{n_p}{n_n + n_p}$$
   where n_p and n_n are the number density of protons and neutrons, respectively.
5. Free energy per baryon: F [MeV].
   The free energy per baryon reads,
   $$f = \varepsilon - Ts.$$

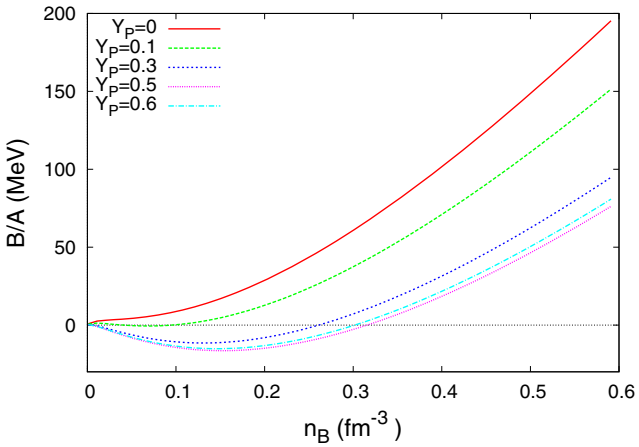

Fig. 4 Binding energy of the nucleons as function of the baryon density with proton fractions Y_p =0, 0.1, 0.3, 0.5, and 0.6

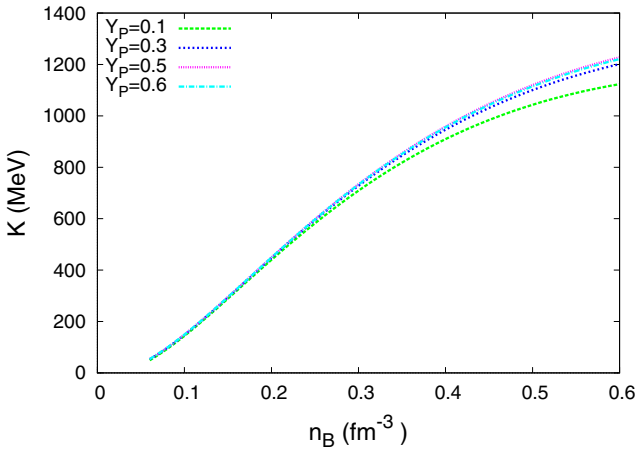

Fig. 5 Compression modulus as function of the baryon density with proton fractions Y_p =0.1, 0.3, 0.5, and 0.6

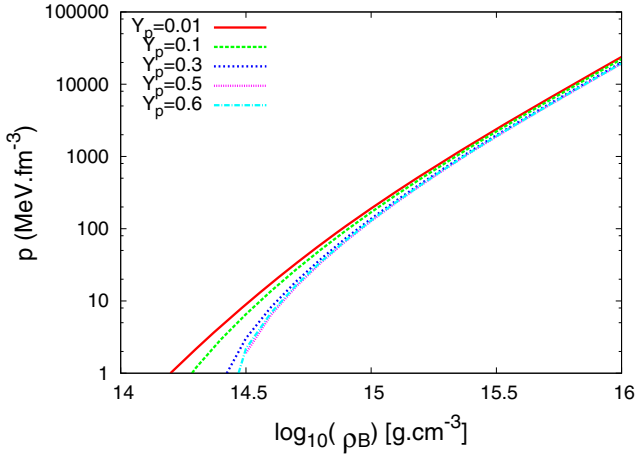

Fig. 6 Pressure as a function of the baryonic density for Y_p =0.01, 0.1, 0.3, 0.5, and 0.6 proton fractions

This work is for zero temperature only, hence $f = \varepsilon$. The free energy per baryon is defined relative to the nucleon mass as,

$$F = \frac{\varepsilon}{n_B} - M = B/A.$$

6. Internal energy per baryon: E_{int} [MeV].
The internal energy per baryon is defined relative to the atomic mass unit $m_u = 931.49432$ MeV as

$$E_{int} = \frac{\varepsilon}{n_B} - m_u.$$

7. Entropy per baryon: $S[k_B]$.
In the present work, temperature is zero and therefore $S = 0$.
8. Effective nucleon mass: M_N^* [MeV].
The effective nucleon mass is obtained in the QMC model for uniform matter with the relation $M_N^* = E_N^{bag}$, where $N = p, n$, and the bag energy is obtained through (7).
9. Free neutron fraction: X_n.
10. Free proton fraction: X_p.
11. Pressure: p [MeV.fm^{-3}].
The pressure is calculated from (10).
12. Neutron chemical potential: μ_n [MeV].
For the zero temperature case, the chemical potential of the neutron relative to the free nucleon mass M reads:

$$\mu_n = [k_n^2 + M^{*2}]^{1/2} + g_\omega \omega_0 - \frac{g_\rho}{2}\rho_{03} - M.$$

13. Proton chemical potential: μ_p [MeV].
For the zero temperature case, the chemical potential of the proton relative to the free nucleon mass M is:

$$\mu_p = [k_p^2 + M^{*2}]^{1/2} + g_\omega \omega_0 + \frac{g_\rho}{2}\rho_{03} - M.$$

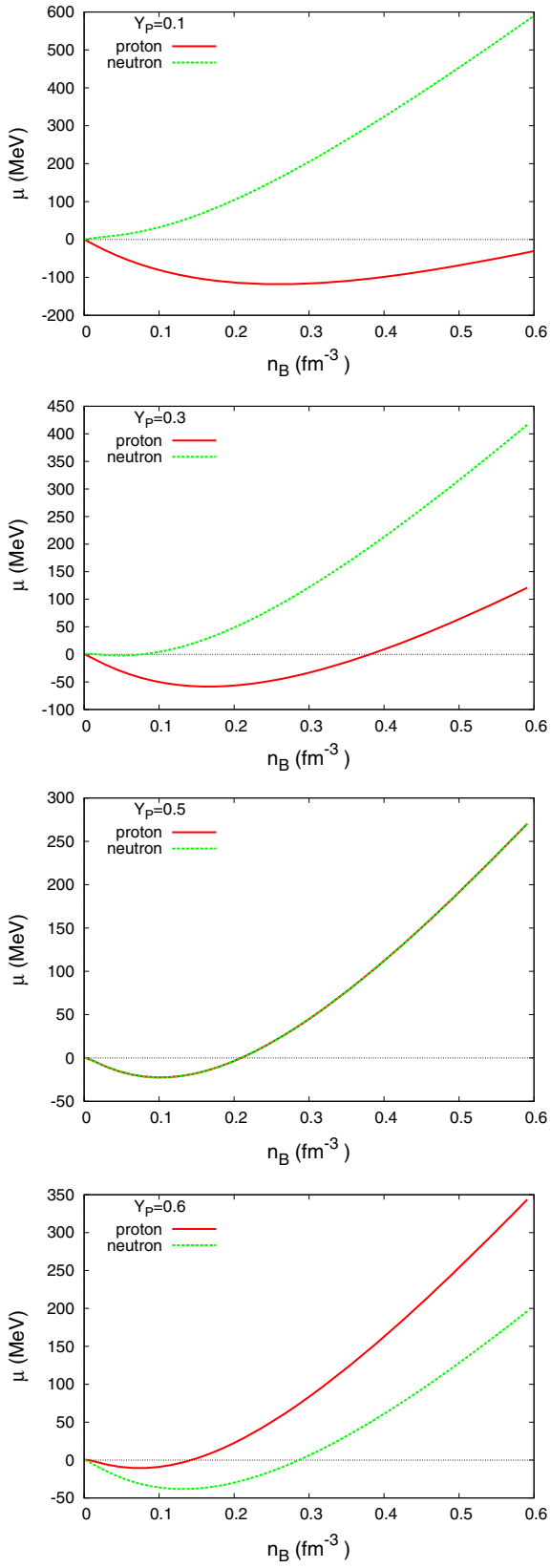

Fig. 7 Neutron and proton chemical potentials as function of the baryonic density. The continuous line represents μ_p and the dashed line represents μ_n

Table 4 EoS table at $T = 0$. It covers the proton fraction range $Y_p = 0-0.65$ with the linear grid spacing $\Delta Y_p = 0.01$ (66 points), and the density range $\rho_B = 10^{14} - 10^{16}$ g cm^{-3} with the logarithmic grid spacing $\Delta \log_{10}(\rho_B/[gcm^{-3}]) = 0.1$ (21 points). This table is available in the website http://debora.fsc.ufsc.br/eos_qmc.t0. An excerpt of it is shown here for guidance

T (MeV)	$\log_{10}(\rho_B)$ $(g.cm^{-3})$	n_B (fm^{-3})	Y_P	F (MeV)	E_{int} (MeV)	S (k_B)	M^*_N (MeV)	X_n	X_p	p $(MeVfm^{-3})$	μ_n (MeV)	μ_p (MeV)
0	14.0	0.0602	0	4.890	12.40	0	838.9	1	0	0.2371	23.43	−68.43
0	14.1	0.0758	0	6.090	13.60	0	816.9	1	0	0.5103	31.20	−82.21
0	14.2	0.0954	0	8.133	15.64	0	791.2	1	0	1.0890	42.68	−97.63
0	14.3	0.1201	0	11.56	19.07	0	761.5	1	0	2.2780	59.66	−114.3
0	14.4	0.1512	0	17.19	24.70	0	728.8	1	0	4.6550	84.64	−131.4

4 Conclusion and Future Works

In this work, we have used the QMC model for the first time to construct an equation of state grid, that in the future can be useful for the studies involving neutron star cooling and supernova simulations. We believe that with the quarks degree of freedom present in the QMC model, the EoS can contribute with part of the physics lacking for SN simulations to explode.

The next step, already under development, is the computation of the EoS grid at finite temperature. Thereafter, we will also study the very low density regions, where nuclear matter is no longer uniform. This will be done with the *pasta phase* approach [52, 53]. We believe that the use of the pasta phase for the description of the non-uniform part of matter that compose the EoS table in the SN simulations will certainly affect SN and cooling simulations.

Finally, we intend to include our complete EoS table in the CompOSE (CompStar Online Supernovae Equations of State) http://compose.obspm.fr data base. With the CompOSE data base, astrophysicists will be able to access a wide range of different EoS, ready for use and all in the same format.

Acknowledgments The authors would like to thank CNPq, grants 300602/2009-0 and 470366/2012-5 and FAPESC under the project 2716/2012, TR 2012000344 for the financial support.

References

1. H.T. Janka, Part, Ann. Rev. Nucl.Sci **62**, 407 (2012)
2. F. Hoyle, W.A. Fowler, Astrophys. J **132**, 565 (1960)
3. A. Burrows, Nature **403**, 727 (2000)
4. J.M. Lattimer, F.D. Swesty, Nucl. Phys. A **535**, 331 (1991)
5. H. Shen et al., Nucl. Phys. A **637**, 435 (1998)
6. H. Shen et al., Astrophys. J. Suppl **197**, 20 (2011)
7. M. Hempel et al., Astrophys. J **748**, 70 (2012)
8. Y. Sugahara, H. Toki, Nucl. Phys. A **579**, 557 (1994)
9. J. Boguta, A.R. Bodmer, Nucl. Phys. A **292**, 431 (1977)
10. J. Boguta, H. Stocker, Phys. Lett **120B**, 289 (1983)
11. G.A. Lalazissis, J. König, P. Ring, Phys. Rev. C **55**, 540 (1997)
12. H. Toki et al., Nucl. Phys. A **588**, 357c (1995)
13. B.G. Todd-Rutel, J. Piekarewics, Phys. Rev. Lett **95**, 122501 (2005)
14. A.W. Steiner, M. Hempel, T. Fischer, Astrophys. J **774**, 17 (2013)
15. F.J. Fattoyev et al., Phys. Rev. C **82**, 055803 (2010)
16. S. Typel et al., Phys. Rev. C **81**, 015803 (2010)
17. M. Hempel, J. Schaffner-Bielich, Nucl. Phys. A **837**, 210 (2010)
18. M. Dutra et al., Phys. Rev. C **90**, 055203 (2014)
19. Y. Sekiguchi et al., Phys. Rev. D **91**, 064059 (2015)
20. S. Nasu et al., Astrophys. J **801**, 78 (2015)
21. E. Abdikamalov et al., Phys. Rev. D **90**, 044001 (2014)
22. C.L. Fryer, A. Heger, Astrophys. J **541**, 1033 (2000)
23. T.A. Thompson, A. Burrows, P.A. Pinto, Astrophys. J. Suppl **592**, 434 (2003)
24. O. Pejcha, T.A. Thompson, Astrophys. J **801**, 90 (2015)
25. R. Buras et al., Phys. Rev. Lett **90**, 241101 (2003)
26. K. Sumyioshi et al., Nucl. Phys. A **730**, 227 (2004)
27. J.M. Lattimer, M. Prakash, Phys. Reports **333–334**, 121 (2000)
28. K. Sumiyoshi et al., Astrophys. J **629**, 922 (2005)
29. P.A.M. Guichon, Lett, Phys. B **200**, 235 (1988)
30. A. Chodos et al., Phys. Rev. D **9**, 3471 (1974)
31. S. Fleck et al., Nucl. Phys. A **510**, 731 (1990)
32. K. Saito, A.W. Thomas, Phys. Lett. B **327**, 9 (1994)
33. K. Saito, A.W. Thomas, Phys. Rev. C **52**, 2789 (1995)
34. P.A.M. Guichon et al., Nucl. Phys. A **601**, 349 (1996)
35. P.K. Panda, D.P. Menezes, C. Providência, Phys. Rev. C **69**, 025207 (2004)
36. P. Demorest et al., Nature **467**, 1081 (2010)
37. J. Antoniadis et al., Science **340**, 6131 (2013)
38. C.H. Johnson, D.J. Horen, C. Mahaux, Phys. Rev. C **36**, 2252 (1987)
39. D. Page, U. Geppert, F. Weber, Nucl. Phys. A **777**, 497 (2006)
40. R. Negreiros, S. Schramm, F. Weber, (2013). arXiv:1307.7692v1 astro-ph 1
41. M. Fortin et al., Phys. Rev. C **82**, 065804 (2010)
42. S.M. de Carvalho et al., (2014). arXiv:1411.5316v1 astro-ph 1
43. A.M. Santos, C. Providência, Phys. Rev. C **79**, 045805 (2009)
44. B.D. Serot, J.D. Walecka, Adv. Nucl. Phys **16**, 1 (1986)
45. N.K. Glendenning, *Compact Stars* (Springer-Verlag, New York, 2000)
46. S. Typel, H.H. Wolter, Nucl. Phys. A **656**, 331 (1999)

47. A.M.S. Santos, D.P. Menezes, Phys. Rev. C **69**, 045803 (2004)
48. S. Weissenborn, D. Chatterjee, J. Schaffner-Bielich, Phys. Rev. C **85**, 065802 (2012)
49. S. Weissenborn, D. Chatterjee, J. Schaffner-Bielich, Nucl. Phys. A **881**, 62 (2012)
50. L.L. Lopes, D.P. Menezes, Phys. Rev. C **89**, 025805 (2014)
51. K.A. Maslov, E. Kolomeitsev, D.M. Voskresensky, (2015). arXiv:1508.03771 astro-ph 1
52. T. Maruyama et al., Phys. Rev. C **72**, 015802 (2005)
53. C. Providência et al., Eur. Phys. J. A **50**, 44 (2014)